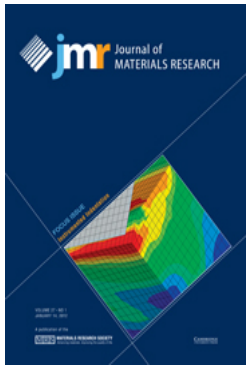

Predation versus protection: Fish teeth and scales evaluated by nanoindentation

Po-Yu Chen, Jeffrey Schirer, Amanda Simpson, Richard Nay, Yen-Shan Lin, Wen Yang, Maria I. Lopez, Jianan Li, Eugene A. Olevsky and Marc A. Meyers

Journal of Materials Research / Volume 27 / Issue 01 / 2012, pp 100 - 112
DOI: 10.1557/jmr.2011.332

Predation versus protection: Fish teeth and scales evaluated by nanoindentation

Po-Yu Chen[a)]
Department of Materials Science and Engineering, National Tsing Hua University, Hsinchu 30013, Taiwan

Jeffrey Schirer, Amanda Simpson, and Richard Nay
Hysitron Inc., Minneapolis, Minnesota 55344

Yen-Shan Lin
Department of Mechanical and Aerospace Engineering, University of California, San Diego, La Jolla, California 92093; and Department of Mechanical Engineering, San Diego State University, San Diego, California 92182

Wen Yang and Maria I. Lopez
Materials Science and Engineering Program, University of California, San Diego, La Jolla, California 92093

Jianan Li
School of Materials Science and Engineering, Shanghai Jiao Tong University, Shanghai 200240, People's Republic of China

Eugene A. Olevsky
Department of Mechanical Engineering, San Diego State University, San Diego, California 92182

Marc A. Meyers
Department of Mechanical and Aerospace Engineering and Department of Nanoengineering, University of California, San Diego, La Jolla, California 92093

(Received 5 May 2011; accepted 26 August 2011)

Most biological materials are hierarchically structured composites that often possess exceptional mechanical properties. We show that nanoindentation can be a powerful tool for understanding the structure-mechanical property relationship of biological materials and illustrate this for fish teeth and scales, not heretofore investigated at the nanoscale. Piranha and shark teeth consist of enameloid and dentin. Nanoindentation measurements show that the reduced modulus and hardness of enameloid are 4-5 times higher than those of dentin. Arapaima scales are multilayered composites that consist of mineralized collagen fibers. The external layer is more highly mineralized, resulting in a higher modulus and hardness compared with the internal layer. Alligator gar scales are composed of a highly mineralized external ganoin layer and an internal bony layer. Similar design strategies, gradient structures, and a hard external layer backed by a more compliant inner layer are exhibited by fish teeth and scales and seem to fulfill their functional purposes.

I. INTRODUCTION

Through hundreds of millions of years of evolution, organisms have developed a myriad of ingenious solutions to ensure and optimize survival and success. Many biological (natural) materials are composites of organic (proteins and/or polysaccharides) and inorganic (minerals) components hierarchically assembled into complex structures at ambient temperature and pressure and usually in an aqueous environment.[1,2] These natural composites have exceptional mechanical properties that are far beyond their relative weak constituents and are often multifunctional and possess self-healing ability. Some examples are abalone nacre,[3,4] crab exoskeletons,[5] chiton radular teeth,[6] and squid beaks.[7] In this study, we investigate teeth and scales from four unique fish species, piranha (Serrasalmus manueli), great white shark (GWS, Carcharodon carcharias), arapaima (Arapaima gigas), and alligator gar (Atractosteus spatula), with emphasis on their microstructure and mechanical properties. The uniqueness is derived from the predatory nature of piranha and shark, on one hand, and extraordinary protection proceeded by the scales of arapaima and alligator gar, on the other.

The design principles of sharp biological materials are reviewed by Meyers et al.[8] Many sharp edges found in plants, insect proboscises, and teeth have serrations which are known to enhance cutting efficiency.[9] Figure 1 shows the structural hierarchy of the cutting mechanisms found in the jaw of a piranha. The jaw is designed with sharp triangular teeth aligned so that as the mouth of the fish

[a)]Address all correspondence to this author.
e-mail: poyuchen@mx.nthu.edu.tw
DOI: 10.1557/jmr.2011.332

closes the initial points of puncture of both the lower and upper jaw are superimposed, as shown in Fig. 1(a). Figure 1(b) is a scanning electron microscopy (SEM) image showing the top view of a piranha tooth. Each tooth exhibits micrometer-sized serrations along its cutting edge, seen in the SEM image of Fig. 1(c). These serrations, approximately 10-15 μm in wave length, are used to create a highly efficient cutting effect, which converts some of the dragging force into normal force at localized points. There is a superimposed compression and shear, which effectively cuts through skin and muscle. As the jaw further closes, any tissues in the trough of the aligned teeth are severed in a guillotine-like confining action. The piranha tooth has two components: the outer layer is identified as enameloid, an enamel-like material composed of rod-shaped hydroxyapatite nanocrystals, and the inner layer is dentin, which consists of mineralized type-I collagen.

The GWS evolved teeth from the scales of its ascendants. It uses these extremely sharp teeth to perform a very specific killing game. To avoid self-injury, the GWS takes one efficiently large bite out of its prey, then retreats and waits for its victim to undergo shock or hemorrhaging before final consumption. This bite takes only one second to complete[10], and the biting stress is measured as high as 600 MPa.[11] Thus, extremely sharp teeth are required. Each tooth is outfitted with a line of large serrations, with up to 300 μm between points. The serrations are perfectly aligned along the cutting edge of the tooth, each creating a mini tooth on the side of its parent tooth. Their shape is close to a hypocycloid. Similar to the piranha tooth, the serrations on this edge maximize the efficiency of the drag force and convert it into points of normal force summed along the side of each serration. Figure 2 shows: (a) an optical image of the overall jaw of a GWS, with multiple rows of teeth, (b) a SEM micrograph of the cutting edge of the tooth with large serrations, and (c) a detailed view of serrations, which have ~300 μm periodicity. Chen et al.[2] compared teeth serration size and body mass of various animals and found that meat eaters, such as the tyrannosaurid dinosaurs, Komodo dragon, and GWS, have serration sizes ranging from 300 to 400 μm, despite the significant difference in body mass and hypothesized that the serration size depends on the mechanical properties of the prey skin and muscle.

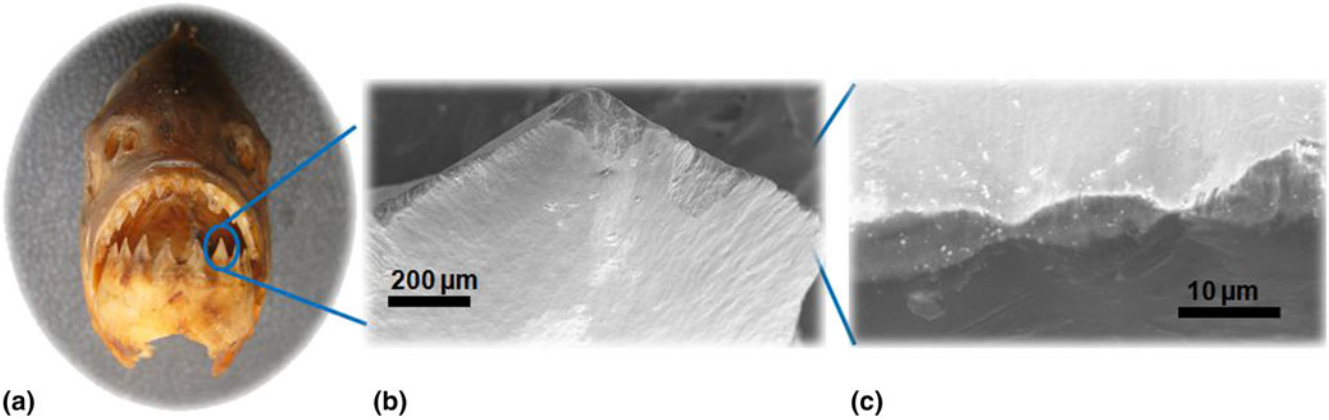

FIG. 1. Hierarchical structure of piranha (Serrasalmus manueli) from jaw to tooth to serrations: (a) photograph showing the jaw of piranha; scanning electron microscopy (SEM) micrographs showing (b) top view of the tooth and (c) detailed view of serrations ~10 μm.

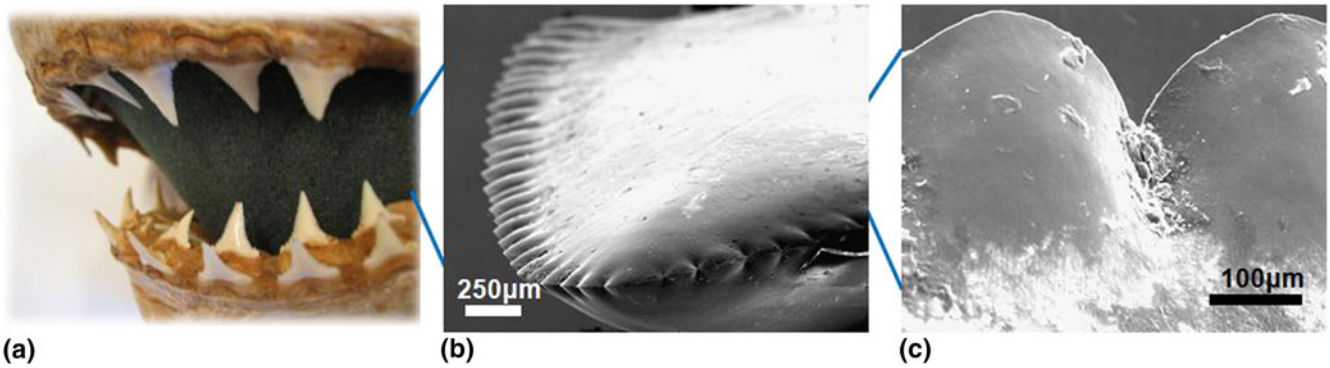

FIG. 2. Hierarchical structure of great white shark (GWS, Carcharodon carcharias) from jaw to tooth to serrations: (a) photograph of the jaw of GWS showing multiple series of dentition; SEM micrographs showing (b) top view of the tooth and (c) detailed view of serrations ~300 μm.

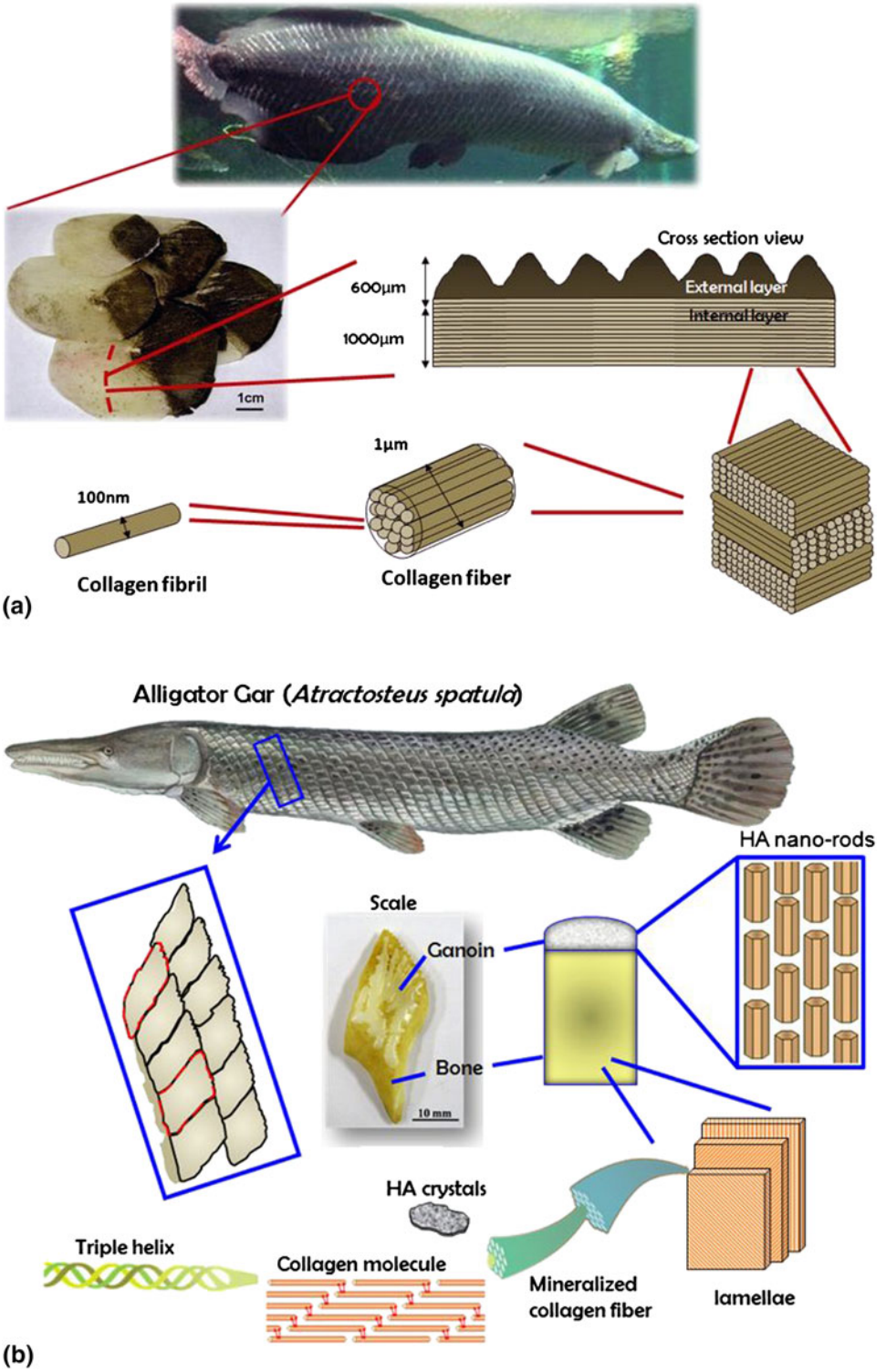

FIG. 3. Hierarchical structure of scales from (a) arapaima (Arapaima gigas) and (b) alligator gar (Atractosteus spatula).

A number of studies on fish scales have been carried out addressing the structural organization, mechanical properties, and design strategies.[12–21] Most fish scales have similar material components to other hard tissues such as bones and teeth, composed mainly of type-I collagen fibers and calcium phosphate-based minerals. Arapaima is one of the largest freshwater fish on earth, reaching a length of about 2–2.5 m and a mass over 150 kg. Arapaima inhabits the Amazon River Basin in South America, coexisting in harmony with the piranha,

fish known for their voraciousness and sharp teeth. It is believed that the scales of Arapaima serve as armor, providing protection against predators.[21,22] Mechanical tests on the scales show that the piranha teeth cannot penetrate the scales.[22] The scales consist of an external layer which is highly mineralized and an internal layer, each 50-60 μm thick and both composed of collagen fibers ~1 μm in diameter. The mineralized collagen fibers form a cross-lamellar arrangement that produces a laminate composite,[18,20] as shown in Fig. 3(a). The microhardness of the external layer (550 MPa) is considerably higher than that of the internal layer (200 MPa), consistent with its higher degree of mineralization.[20] The scale can be considered as a functionally graded material: the internal layer provides flexibility and toughness while the external layer gives required hardness and wear resistance for protection.

The alligator gar is the largest freshwater fish found in North America, measuring up to 3 m and weighing up to 100 kg at maturity. Its size rivals the Arapaima. The scales are diamond-shaped with serrated edges, which can be used to cut potential predators [Fig. 3(b)]. The scales consist of a highly mineralized external layer of ganoin, which is known to be an enamel-like mineral with hydroxyapatite nanorods,[23] and an internal bony layer made of highly mineralized collagen fibers. Native Americans and swamp inhabitants use alligator gar scales as jewelry.

Probing the mechanical properties of biological materials such as fish teeth and scales is challenging due to their relative small size and complex multilayered structure. Nanoindentation has become a powerful technique that is capable of probing the mechanical properties at micro- and nanometer length scales with high resolution, spatially specific accuracy.[24] In recent years, this new technique has been widely applied to studies of bone,[25–29] cartilage,[30–32] and teeth,[33–37] and extensively reviewed by several groups.[38–45] There are many considerations to take into account when determining mechanical properties of biological materials by

TABLE I. User-specified parameters for nanoindentation testing on all specimens.

Specimen	Region of interest	Indent pattern	Peak indentation load (μN)	Indent spacing (μm)	Total number of indents[a]
Piranha tooth	Entire cross section	Grid	1000	50	699
Piranha tooth	Dentin–enameloid junction (DEJ)	Grid	500	8	340
Piranha tooth	DEJ	Line profile[b]	300	2-3	42
Piranha tooth	Enameloid (hydrated)	User-defined[b]	1000	4-6	20
Piranha tooth	Dentin (hydrated)	User-defined[b]	1000	4-6	20
Great white shark (GWS) tooth	Entire cross section	Grid	1000	100	753
GWS tooth	DEJ	Grid	500	20	400
GWS tooth	DEJ	Line profile[b]	300	2-3	47
GWS tooth	Enameloid (hydrated)	Grid	1000	5-6	20
GWS tooth	Dentin (hydrated)	Grid	1000	5-6	20
Gar scale	Entire cross section	Grid	500	25	2541
Arapaima scale	Entire cross section	Line profile	500	10	371

[a]Outermost (extreme) curves were removed from analysis but are included in the total number of indents performed per specimen location
[b]User-defined indent locations specified from SPM images

TABLE II. Reduced modulus and hardness measured from nanoindentation.

Specimen	Area	Condition	Reduced modulus (GPa)	Hardness (GPa)
Great white shark (GWS)	Enameloid	Ambient (dry)	84.4 ± 19.9	4.1 ± 1.1
GWS	Enameloid	Hydrated	77.2 ± 14.8	2.6 ± 0.9
GWS	Dentin	Ambient (dry)	20.4 ± 5.6	0.7 ± 0.2
GWS	Dentin	Hydrated	8.7 ± 3.1	0.2 ± 0.1
Piranha	Enameloid	Ambient (dry)	86.5 ± 15.9	4.1 ± 0.9
Piranha	Enameloid	Hydrated	81.9 ± 8.4	3.1 ± 0.4
Piranha	Dentin	Ambient (dry)	23 ± 6.0	0.8 ± 0.3
Piranha	Dentin	Hydrated	12.4 ± 1.6	0.2 ± 0.04
Gar	External	Ambient (dry)	70.8 ± 4.5	3.6 ± 0.3
Gar	Internal	Ambient (dry)	20.5 ± 2.4	0.7 ± 0.1
Arapaima	External	Ambient (dry)	33.7 ± 3.7	1.3 ± 0.2
Arapaima	Internal	Ambient (dry)	15.7 ± 5.1	0.5 ± 0.2

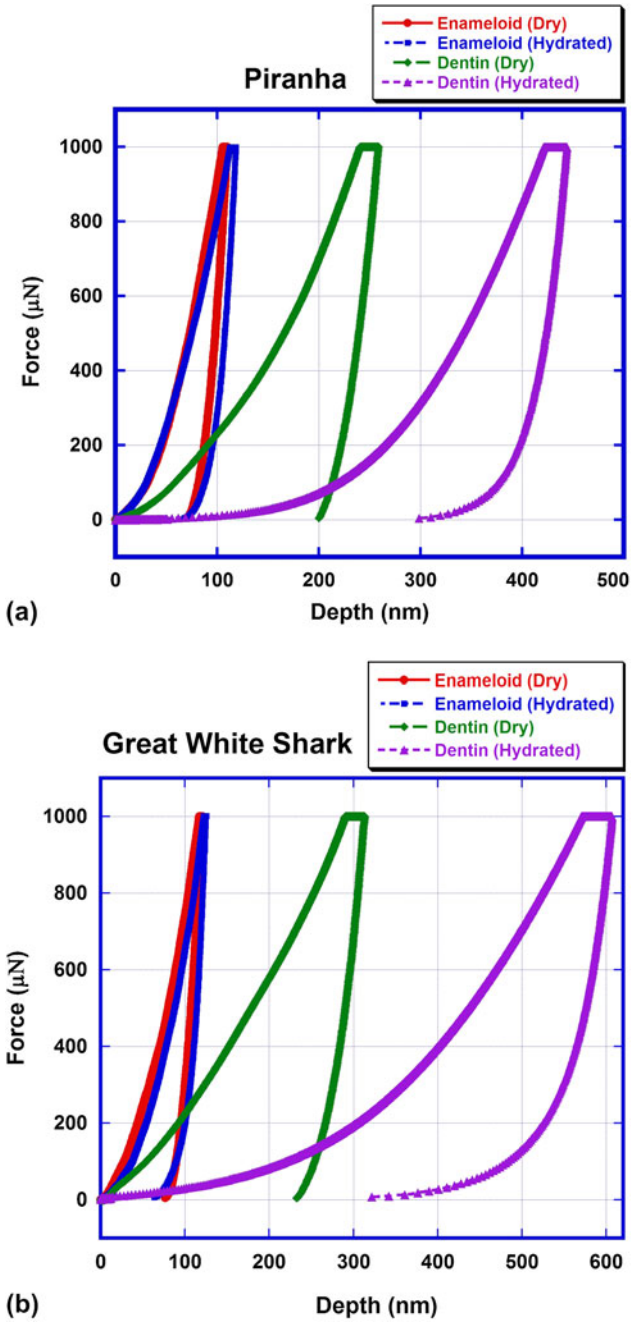

FIG. 4. Representative force-depth curves of enameloid and dentin from (a) piranha and (b) GWS tested in ambient dry and hydrated conditions.

nanoindentation, such as the effects of viscoelasticity, adhesion, tip selection, storage medium, and sample preparation. Many biological materials exhibit viscoelastic or time-dependent mechanical behavior. The elastic modulus of human cortical bone obtained from the quasi-static nanoindentation tests increased with the indentation loading rate and strain rate.[29] The effects of time-dependent plasticity can be diminished by multiple loading-unloading cycles followed by a long holding period at maximum load before final unloading.[29] Additionally, the samples can be tested in a dynamic mode, where sinusoidal loads can be applied to measure storage and loss modulus as a function of loading frequency. Most biological materials are naturally hydrated and hydration plays an important role in mechanical properties. Studies on human cortical bone showed that the elastic modulus measured by nanoindentation increased 11–28% after dehydration.[27,28] Habelitz et al.[37] investigated changes in mechanical properties of human dentin and enamel during storage in deionized (DI) water, calcium chloride-buffered ($CaCl_2$) saline solution, and Hank's Balanced Salt Solution (HBSS). Results showed that the elastic modulus and hardness of dentin and enamel decreased significantly when storing in DI water or $CaCl_2$ solution, while there was no significant change in mechanical properties when storing the specimens in HBSS. A recent study by Dickinson[44] compared the effect of three storage solutions [DI water, HBSS, and phosphate buffered saline(PBS)] on the mechanical properties of human enamel, dentin, and bone. The results showed that storage of mineralized tissues in any of these solutions can significantly (>70%) reduce their mechanical properties possibly due to demineralization. The study indicated the importance of testing biological tissues immediately after extraction.

In this study, we focus on nanomechanical properties of fish teeth and scales using advanced nanoindentation techniques and compare the results with those previously obtained from microindentation and bulk mechanical tests. Comparisons between two types of fish teeth and scales are also made, and the effect of hydration on mechanical properties is discussed.

II. MATERIALS AND METHODS

A. Sample preparation

The piranha teeth and arapaima scales were acquired from the Araguaia River (Amazon Basins) in Brazil. The GWS teeth were obtained from Del Mar, CA, and the alligator gar scales were donated by Dianne Ulery (Dianne Ulery's Natural Jewelry Art, Alexandria, LA, website: http://www.bonanza.com/Dianne_Ulery). All samples were kept in ambient dry condition before testing. The period of time between the teeth and scales being removed from the animals and tested mechanically was approximately 6 months. For each of the four species, samples were obtained from one animal. Two front teeth were sectioned transversely approximately half way down the cusp from the upper jaws of shark and piranha. The arapaima and alligator gar scales were obtained from the central region of the fish body. Two small pieces (20 mm × 5mm × 2 mm) were cut from the dark (exposed) region from an arapaima scale. For the alligator gar, two

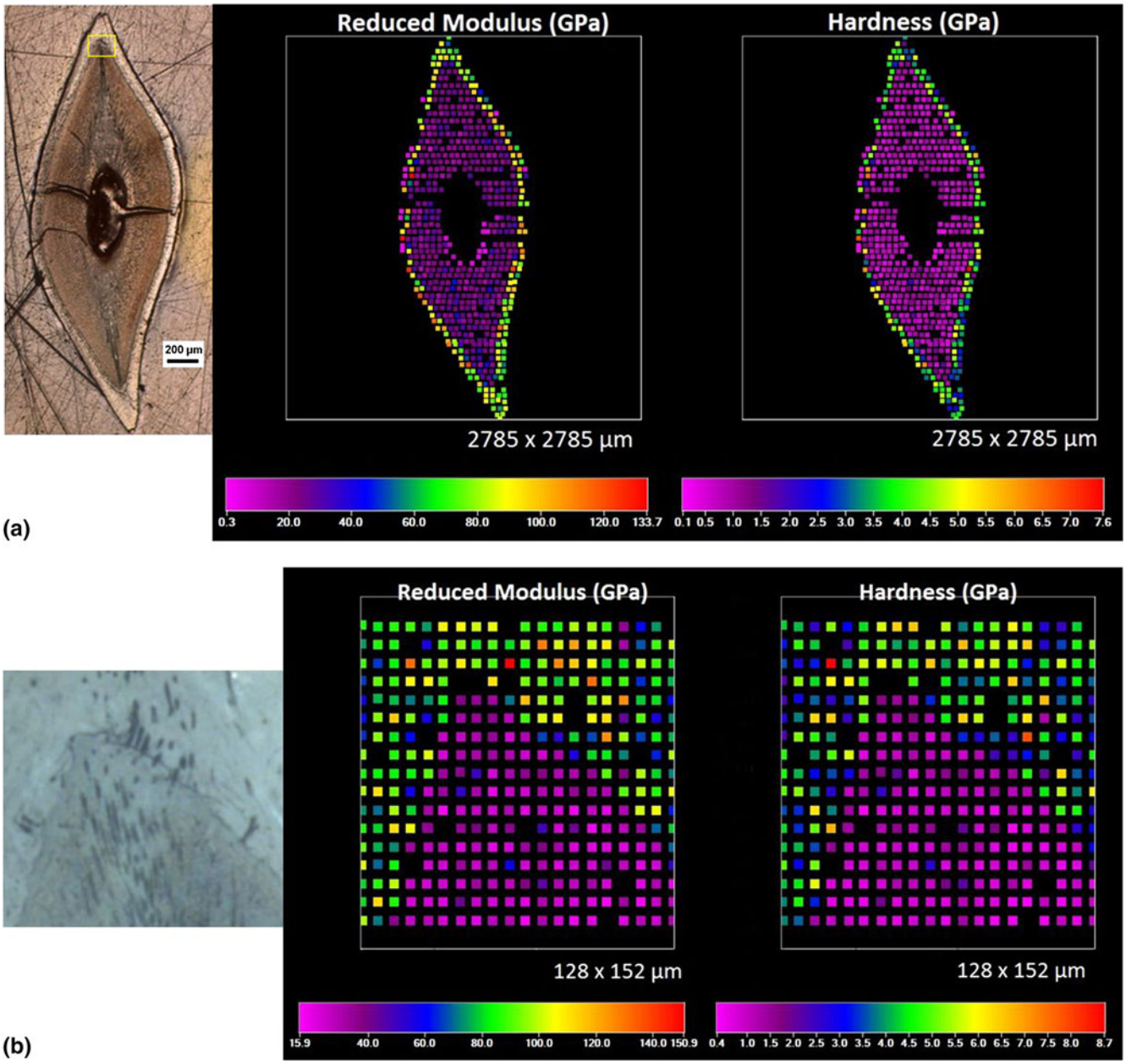

FIG. 5. (a) Reduced modulus and hardness maps of cross-sectional area in a piranha tooth; (b) zoom-in modulus and hardness maps (128 μm × 152 μm) at the dentin-enameloid junction (DEJ) region.

specimens were made by cutting a scale in half using a diamond rotating blade through the long axis. All samples were mounted in epoxy with cross-sectional area revealed, followed by grinding and fine polishing.

B. Structural characterization

Optical micrographs of polished samples were taken using a Zeiss Axio imager (Zeiss MicroImaging Inc., Thornwood, NY) equipped with a CCD camera in the reflective light mode. The microstructure was characterized by using a field emission scanning electron microscope (FEI-XL30, FEI Company, Hillsboro, OR). Samples prepared for SEM were mounted on aluminum sample holders and sputter coated with a thin layer of gold.

C. Nanoindentation

Nanoindentation testing was performed using a TI-950 TriboIndenter (Hysitron Inc., Minneapolis, MN). User-specified parameters for testing each sample are summarized in Table I. Each indent took ~90 s to complete. Depending on the total number of indents, the tests took from 30 min to 18 h. The testing temperature was 24 °C

and the relative humidity was 15% when testing in the ambient dry condition. The nanoindentation instrumentation enclosure ensured that the temperature and humidity were kept fairly constant throughout the testing and no effect was noticed with time.

For relatively large areas (on the order of hundreds of microns to several millimeters), regions for testing were identified using an optical microscope integrated into the nanoindentation system. Subsequent grids of indents were performed on specified locations with user-specified peak loads and indent spacing. For smaller areas (less than 100 μm), regions for testing were identified using scanning probe microscopy (SPM), utilizing the nanoindentation tip as the SPM probe to obtain pretest in-situ SPM images. In-situ SPM imaging provided significant information on sample surface morphology on piranha and GWS specimens, which helped to identify desired test regions [dentin-enameloid junction (DEJ)]. Prior to the measurements, preliminary indents were performed in each region and the size of the residual indent was measured. The peak loads were chosen for different testing conditions to give proper spacing between the indents. For example, the indents in the line profile that were user-defined using SPM imaging were spaced close together, so a lower force (300 μN) was required to not have overlapping elastic and plastic zones. The indents in the DEJ grid were spaced farther apart, so a load of 500 μN was used. A peak force of 1000 μN was applied to probe the mechanical properties throughout the entire cross section of the specimen. In this case, the adjacent indents were spaced 50 or 100 μm apart.

For GWS and piranha specimens, a diamond fluid cell Berkovich probe was utilized to perform tests in both ambient (dry) and hydrated conditions. Samples were immersed in a D-PBS solution during hydrated testing, with a minimum of 2 h of hydration time prior to testing. The measurements were performed in fluid immediately after the samples were fully hydrated to prevent demineralization and degradation of mineralized tissues in solutions, which may affect the mechanical properties. The series of indents were accomplished within 1 h and no physical change of the sample, such as swelling was observed. Tests on GWS and piranha samples were performed in load-controlled feedback mode to various peak forces. A load function consisting of a 5-s loading to peak force segment, followed by a 5-s hold segment, and a 1-s unloading segment was used. For gar and arapaima specimens, a diamond Berkovich probe was utilized to perform load-controlled tests in ambient (dry) conditions. A load function consisting of a 5-s loading to peak force segment, followed by a 2-s hold segment, and a 5-s unloading segment was used. Nanoindentation hardness and reduced modulus (in GPa) were calculated based on the well-established Oliver-Pharr method for nanoindentation testing.[24]

III. RESULTS AND DISCUSSION

A. Piranha teeth

The reduced modulus and hardness (mean ± SD) of the four types of fish samples measured by nanoindentation are summarized in Table II. Figure 4(a) shows representative force-depth curves of piranha enameloid and dentin tested in ambient dry and hydrated conditions. When tested in ambient dry condition, the enameloid of the piranha tooth has a mean reduced modulus of 86.5 ± 15.9 GPa and a mean hardness of 4.1 ± 0.9 GPa, while dentin

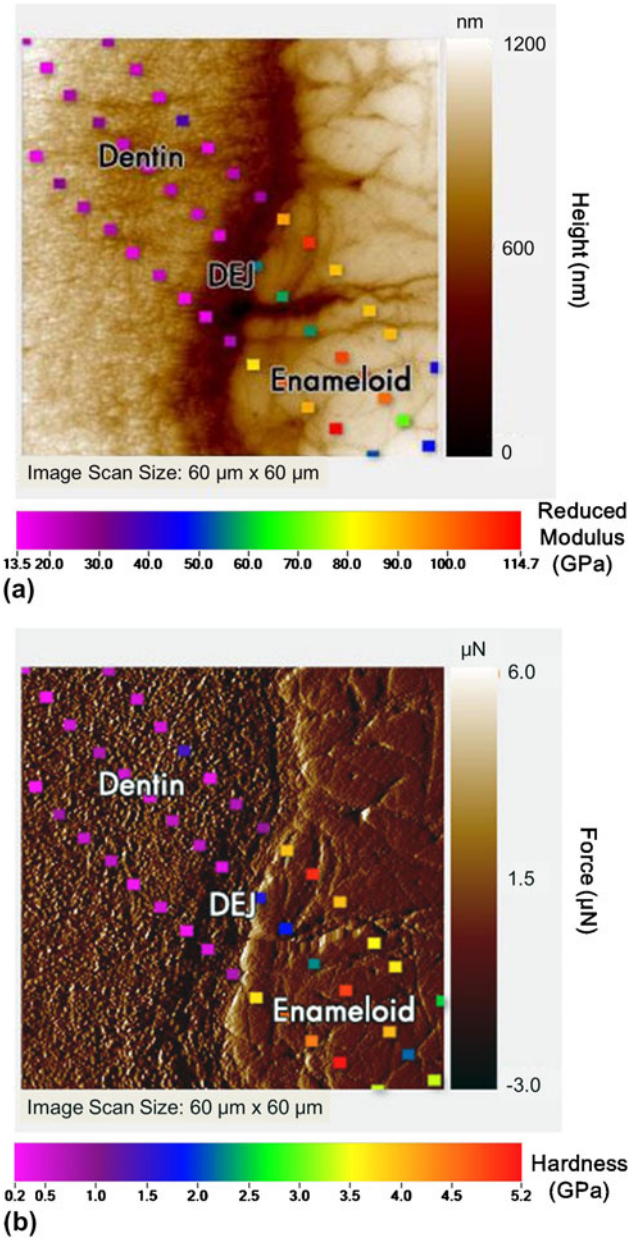

FIG. 6. (a) Reduced modulus results overlay on the topographical scanning probe microscopy (SPM) image; (b) Hardness values overlay on the gradient SPM image at the DEJ region of piranha (60 μm × 60 μm).

has a mean reduced modulus and hardness of 23.0 ± 6.0 and 0.8 ± 0.3 GPa, respectively. The dentin and enameloid were further tested in hydrated condition to understand the effect of hydration on the mechanical properties of dentin and enameloid. The modulus and hardness (81.9 ± 8.4 and 3.1 ± 0.4 GPa) of enameloid in hydrated condition are lower compared with those tested in dry condition and those of hydrated dentin are significantly reduced to 12.4 ± 1.6 and 0.2 ± 0.04 GPa. Enameloid is a highly mineralized tissue with very small amount of organic component and water (<5%) compared with dentin. Thus, the effect of hydration on the mechanical properties of enameloid is not as significant as in dentin. Demineralization of mineralized tissues in solutions is

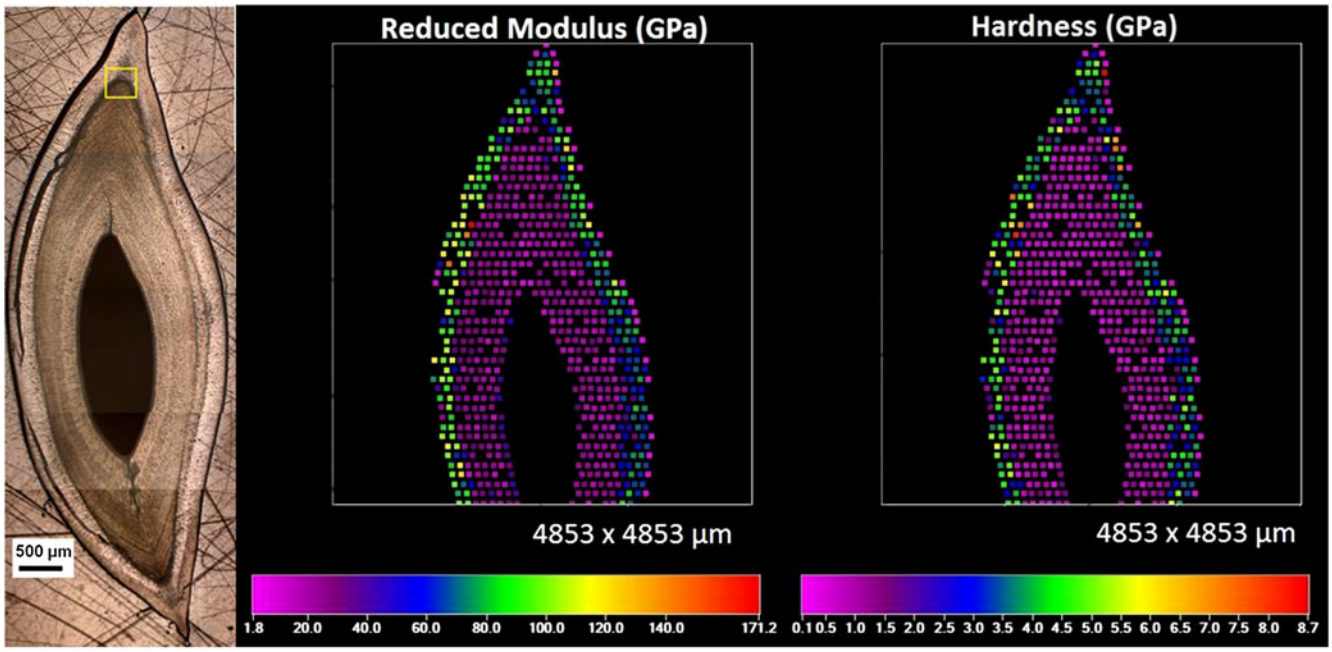

(a)

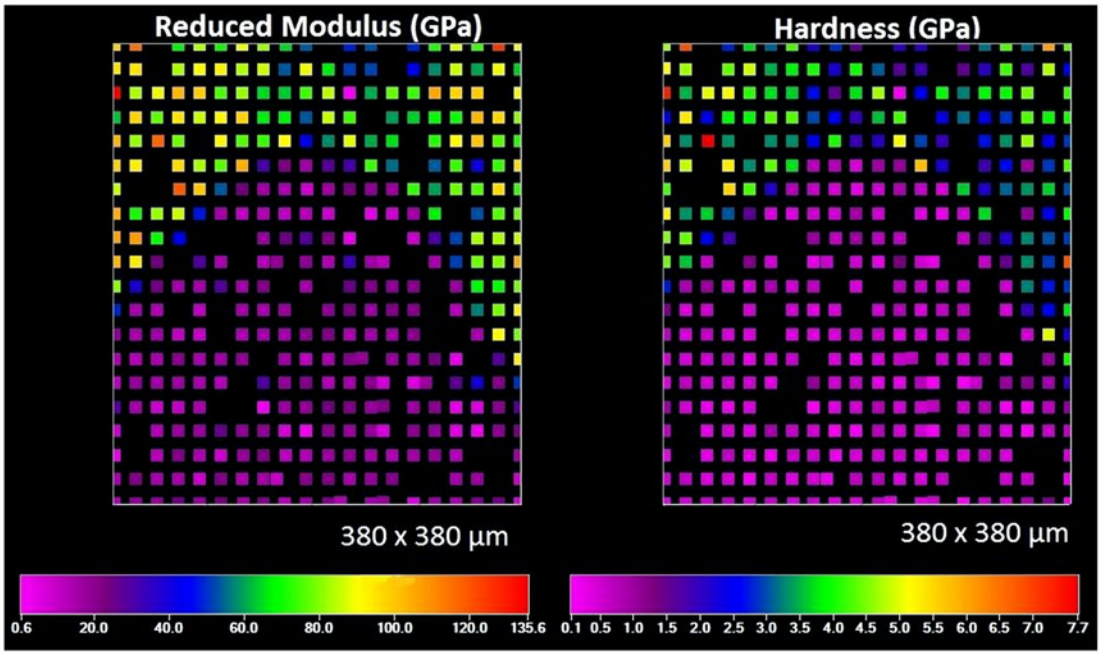

(b)

FIG. 7. (a) Reduced modulus and hardness maps of cross-sectional area in a GWS tooth; (b) zoom-in modulus and hardness maps (380 μm × 380 μm) at the DEJ region.

certainly expected, and the first 12-24 h are crucial. Thus, the samples were tested immediately after full rehydration to minimize the effects of demineralization and degradation. Although it is known that HBSS might be a better storage medium for teeth (particularly for dentin)[37] compared with PBS which is generally better for bone, the effects of the storage medium on the mechanical properties should not be significant since the samples were kept in the solution for a relatively short period of time (less than 4 h). The hardness values measured from nanoindentation are twice as high as those previously measured by microindentation (enameloid ~1.5 GPa, dentin ~0.3 GPa).[2,21] This is due to the size effect: the frequency of weak links (cracks, ligaments, voids, interfaces) decreases with decreasing size, leading to higher hardness. This was expressed quantitatively by Yao and Gao[46] in their hierarchical structure (Russian doll) theory.

Figure 5(a) shows an optical micrograph of the cross-sectional area in a piranha tooth along with reduced modulus and hardness maps in color scale. It is clearly seen that the external enameloid layer has much higher modulus and hardness compared with internal dentin. A condensed grid of indents (17 × 20, 8 μm apart) was performed at the DEJ of piranha to measure the local mechanical properties at the junction. The zoom-in modulus and hardness maps (128 μm × 152 μm) at the DEJ are shown in Fig. 5(b). Lines of indents (2-3 μm apart) were performed along the DEJ of the piranha sample in order to take an even closer look at the mechanical properties along the junction. Figures 6(a) and 6(b) show topographical and gradient in-situ SPM images of the DEJ area (60 μm × 60 μm) where the indents were performed. Reduced modulus and hardness values were overlaid on the topographical and gradient in-situ SPM images, respectively, and the difference in mechanical properties between dentin and enameloid can be clearly seen. It should be noted that the peak indentation loads varied from 300 to 1000 μN depending on different testing conditions and locations, as shown in Table I. The loading time was kept the same (5 s) so that the loading rate varied from 60 to 200 μN/s. Fan and Rho[29] investigated the effects of viscoelasticity on nanoindentation measurements of human cortical bone and found that the elastic modulus increased with loading rate. However, the effect of loading rate on the mechanical properties of dentin and enameloid should be minor since the magnitude of the loading rate differences in our nanoindentation measurements is only a factor of 3.

Nanoindentation measurements were performed to map mechanical properties of a piranha tooth at varying length scales, from an entire cross-sectional area, a smaller area enclosing dentin and enameloid, to a more localized region at the DEJ. The space between adjacent indents for nanoindentation ranges from 3 to 50 μm, much smaller compared with that for microindentation, which often reaches ~200 μm. A limited amount of data points can be obtained using microindentation on small biological samples with a complex microstructure, such as piranha teeth, making nanoindentation a suitable and superior testing method over microindentation.

B. GWS teeth

A cross-sectional optical micrograph of a GWS tooth and corresponding modulus and hardness maps are shown in Fig. 7(a). Higher resolution modulus and hardness maps at the DEJ region are shown in Fig. 7(b). Similar to the piranha, the significant difference in mechanical properties between enameloid and dentin can be clearly seen. The reduced modulus and hardness of shark enameloid tested in ambient dry condition are 84.4 ± 19.9 and 4.1 ± 1.1 GPa, and those of shark dentin are 20.4 ± 5.6 and 0.7 ± 0.2 GPa, respectively. Figure 4(b) shows representative force-displacement curves of shark

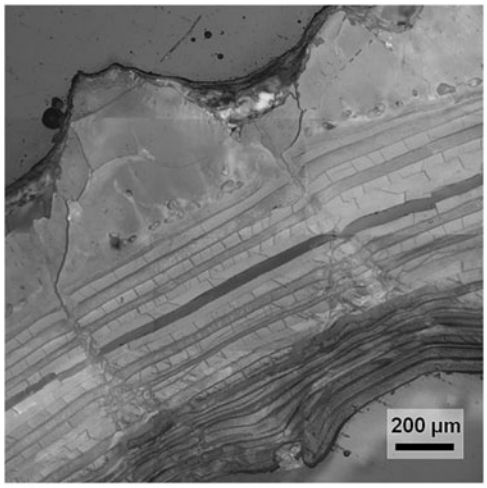

(a)

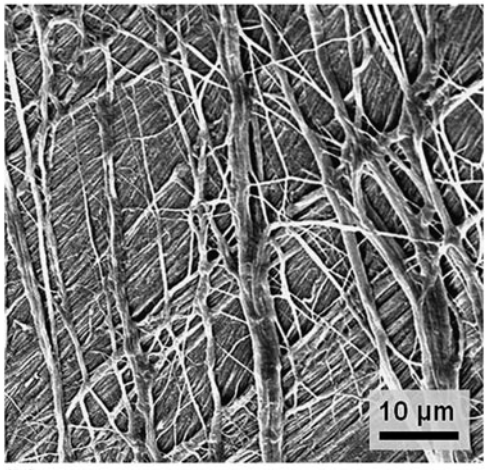

(b)

FIG. 8. (a) Optical micrograph showing the external and internal layers in the scale of Arapaima gigas; (b) SEM image showing the orientation of collagen fibers in adjacent layers.

enameloid and dentin tested in ambient dry and hydrated conditions. When tested in the hydrated condition, the modulus and hardness of shark enameloid reduce to 77.2 ± 14.8 and 2.6 ± 0.9 GPa, while those of shark dentin drop more drastically to 8.7 ± 3.1 and 0.2 ± 0.1 GPa, respectively. The mechanical properties of dentin and enameloid of shark tooth and the effect of hydration are in good agreement with those of piranha tooth. Whitenack et al.[47] investigated mechanical properties of teeth from two types of sharks, the sand tiger shark (Carcharias taurus) and the bonnethead shark (Sphyrna tiburo), using nanoindentation in dry condition. The reduced modulus and hardness of tiger shark enameloid are 72.61 ± 4.73 and 3.20 ± 0.20 GPa, and those of bonnethead shark enameloid are 68.88 ± 1.50 and 3.53 ± 0.30 GPa, respectively. The tiger shark dentin has reduced modulus and hardness of 28.44 ± 2.21 and 1.21 ± 0.16 GPa, and the bonnethead shark dentin has reduced modulus and hardness of 22.49 ± 1.72 and 0.97 ± 0.07 GPa, respectively. The reported mechanical properties of the tiger and bonnethead sharks are in good agreement with those of the GWS in this study.

Despite that the GWS and piranha are significantly different in taxonomy, habitat, body size, and morphology, the microstructure and mechanical properties of their teeth are similar. Both GWS and piranha teeth consist of highly mineralized enameloid and dentin, which is made of mineralized collagen fibrils. Mechanical properties of GWS and piranha measured from nanoindentation are comparable, as shown in Table II. The reduced modulus and hardness of enameloid are 4-5 times higher than those of dentin when tested in ambient dry condition. The difference in mechanical properties between enameloid and dentin is more significant (7-15 times) when tested in rehydrated condition. Imbeni et al.[48] studied the critical role of dental-enamel junction in enhancing fracture resistance of human teeth. SEM observation showed that

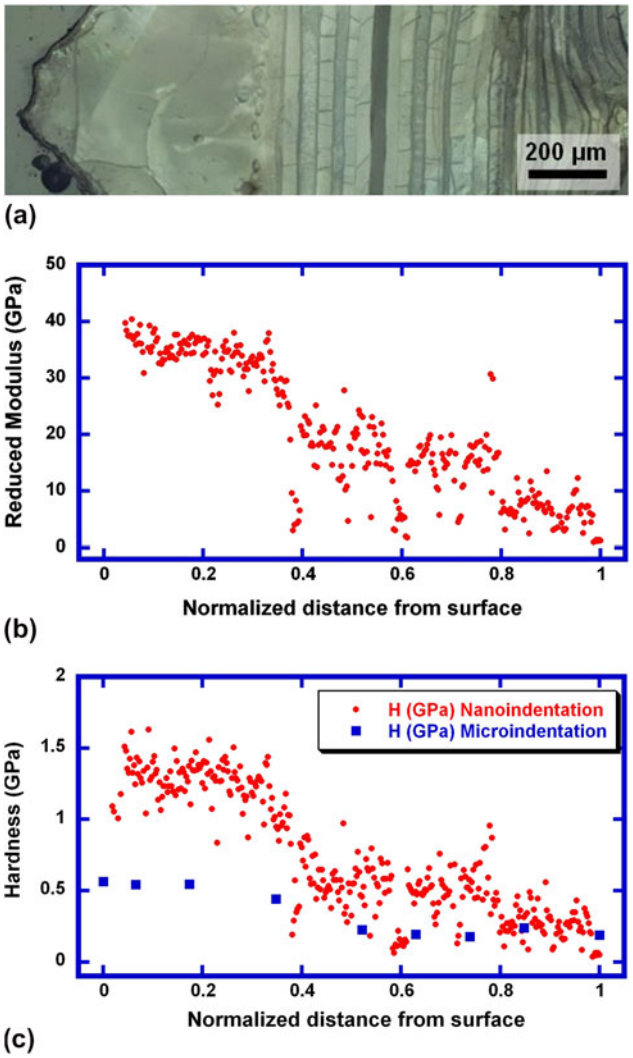

FIG. 9. (a) Cross-sectional optical micrograph showing region where nanoindentation was performed for arapaima scale; (b) reduced modulus and (c) hardness through the thickness of scale. The hardness values measured from nanoindentation are compared with those measured from microindentation.[20]

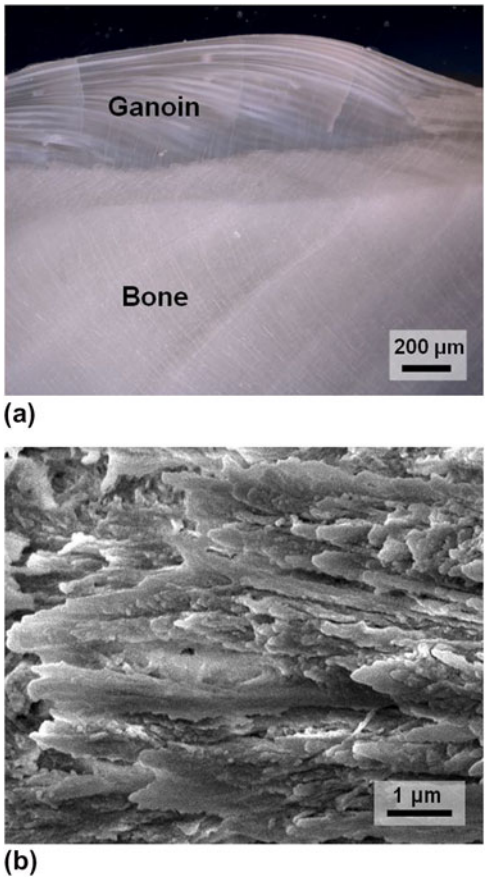

FIG. 10. (a) Optical micrograph showing the cross-sectional area of an alligator gar scale, which consists of two regions, external ganoin layer and internal bony layer; (b) SEM images showing fracture surface of mineralized collagen fibers in the internal bony layer.

cracks initially formed in enamel tend to penetrate the DEJ and stop when they enter the tougher dentin adjacent to the interface due to extrinsic toughening mechanisms such as uncracked ligament bridging. Such design, i.e., hard and brittle external enameloid enclosing softer and tougher dentin, provides enhanced mechanical properties that are required to fulfill functional purposes.

C. Arapaima gigas scales

Figure 8(a) is a cross-sectional optical micrograph showing the external and internal layers of an Arapaima scale. The corrugated surface of the external layer corresponds to the ridge structure seen on the surface, whereas the internal layers are characterized by lamellae. Figure 8(b) is a top-view SEM image showing the collagen fiber orientation between two adjacent layers, which has an angle of ~75°. Figure 9(a) is an optical micrograph showing the cross-sectional hardness mapping through the thickness of an arapaima scale. Figures 9(b) and 9(c) show the reduced modulus and hardness variation through the scale, from the external layer to the internal layer. The reduced modulus measured at the external layer is 33.7 ± 3.7 GPa and gradually decreasing to 15.7 ± 5.1 GPa in the internal layer. The hardness shows the same trend, decreasing with distance from the external layer (1.3 ± 0.2 GPa) to the internal layer (0.5 ± 0.2 GPa). The results are in accord with the calcium and phosphorous mapping through the scale thickness previously reported by Lin et al.[20] The external and internal layers are both composed of mineralized collagen fibers, yet the external layer has higher mineral content than the internal one. As a result, the external layer has higher hardness and modulus than the inner layer. Lin et al.[20] performed microindentation across the scale. The reported hardness of the outer layer was found to be ~550 MPa and that of the inner layer was ~200 MPa [Fig. 9(c)], much lower than the nanoindentation hardness in this study. The significant difference may attribute to that the microhardness tests were performed in rehydrated condition while the nanoindentation measurements were carried out in ambient dry condition. The harder external layer is ideal to serve as protective armor against the sharp teeth of predators and such functional design is widely found in nature, e.g., a hard exocuticle covering endocuticle in crab shells.[5] Meyers et al.[21] performed penetration tests of piranha teeth into arapaima scales simulating the vigorous piranha bite. Results show that the piranha teeth cannot penetrate the exposed portion of arapaima scales. The piranha teeth fractured and embedded in the scales before further penetration. The highly mineralized external layer of scales plays a key role in protecting arapaima from being attacked by piranha.

D. Atractosteus spatula scales

Figure 10(a) is an optical micrograph showing the cross-sectional area of an alligator gar scale, which

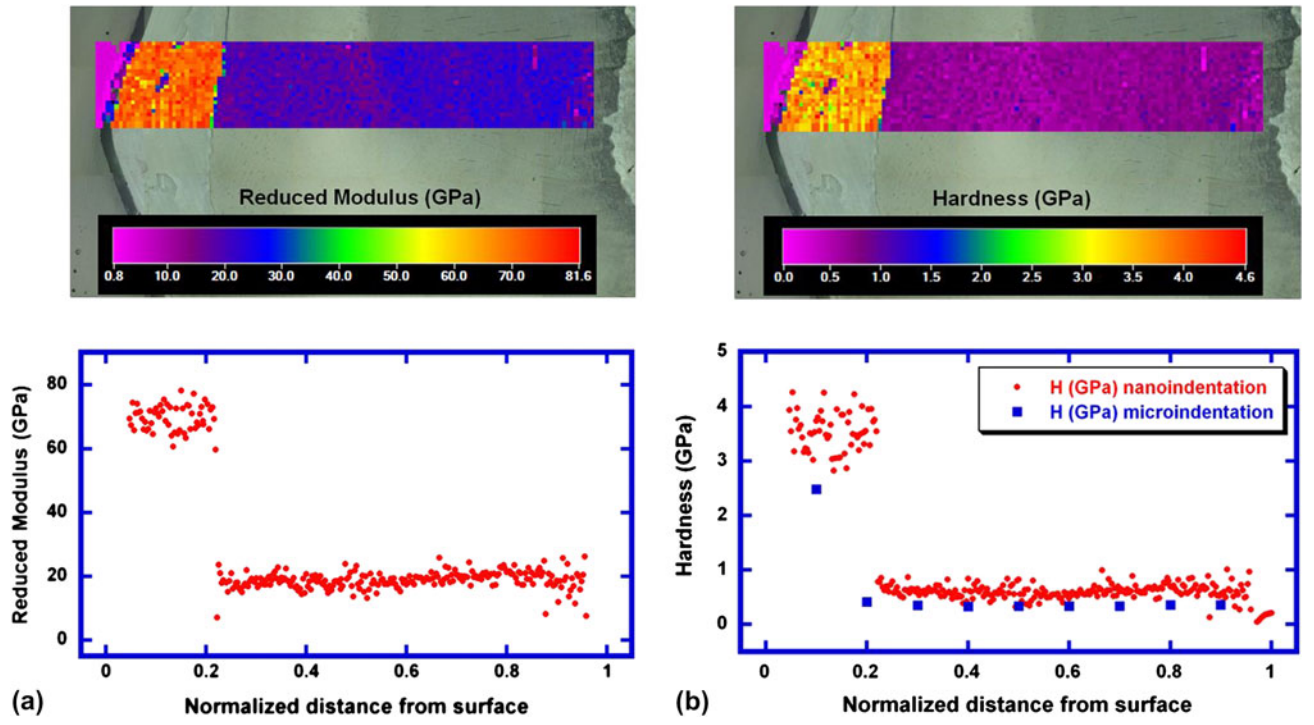

FIG. 11. Cross-sectional optical micrograph overlapped with (a) reduced modulus and (b) hardness maps through the thickness of an alligator gar scale. The hardness values measured from nanoindentation are compared with those measured from microindentation tests.

consists of two regions; an external ganoin layer and an internal bony layer. Figure 10(b) is a SEM image showing the mineralized collagen fibers in the internal bony layer. Figure 11(a) shows the reduced modulus map through the thickness of the gar scale. The modulus measured at the external ganoin layer is 70.8 ± 4.5 GPa and that in the internal bony layer drops to 20.5 ± 2.4 GPa. The modulus of ganoin is comparable to that of enameloid in the fish teeth and that of bony layer is in good agreement with the elastic modulus of bone.[25–27] Unlike the gradual change in mechanical properties found in arapaima scales, there is a distinct interface between ganoin and bony layers, which is akin to the DEJ. The hardness of the ganoin layer is 3.6 ± 0.3 GPa and that of bony layer is 0.7 ± 0.1 GPa, as shown in Fig. 11(b). Hardness values measured from microindentation are lower compared with those obtained by nanoindentation. The external ganoin layer has a microhardness of 2.5 GPa, whereas the bony layer has a microhardness of 0.35 GPa. Bruet et al.[17] found that the scales from *Polypterus senegalus* have four layers: ganoin, dentin, isopedine, and bony layers (from external to internal regions). Here, two regions (ganoin and bony layers) are found in alligator gar scales. The modulus (~62 GPa) and hardness (~4.5 GPa) of the outer ganoin layer and those of inner bony layer ($E \sim 17$ GPa, $H \sim 0.54$ GPa) of *Polypterus senegalus* scales are consistent with our results. The hard, highly mineralized ganoin layer is designed for protection from predator's attack, and the underlying, more compliant bony layer dissipates energy and provides flexibility of the entire fish body. The multilayered structure and graded mechanical properties seem to be widely adopted in fish scales and biological armor materials, indicating evidence of evolutionary convergence which may inspire the design of novel composites.[49,50]

IV. CONCLUSIONS

In this study, we investigated the mechanical properties of two types of fish teeth (piranha and GWS) and two types of fish scales (arapaima and alligator gar) using advanced nanoindentation techniques and compared our results with previous microindentation tests. These biological materials provide superior predatory capability (teeth) and protection (scales) in fish and therefore their mechanical properties are essential. Nanoindentation provides position-specific and high-resolution information of mechanical properties, which can probe the nano and microstructure of biological materials. Despite the diversity between fish species, similar design strategies are found in teeth and scales. All samples have a hard, highly mineralized external layer and a tough, less mineralized internal layer. The enameloid in fish teeth is 4-5 times harder than the dentin. Similar trends are found in the ganoin and bony layers in alligator gar scales as well as the arapaima scales.

The piranha and GWS teeth were further tested in a hydrated condition. The results show that hydration has a strong effect on the mechanical properties of dentin, while no significant difference is observed in the highly mineralized, collagen-deficient enameloid. This study demonstrates that nanoindentation is indeed a powerful technique for probing and elucidating mechanical properties of biological materials, which usually have a complex hierarchical structure and multifunctionality ranging in many length scales.

ACKNOWLEDGMENTS

We thank Ryan Anderson (CalIT^2) for the help on the scanning electron microscopy. Valuable insights and discussion with Ms. Dianne Ulery are greatly appreciated. She kindly donated the alligator gar scales for research purposes. We thank Professor Joanna McKittrick for her enthusiastic support of this project. This research is funded by the National Science Foundation, Division of Materials Research, Biomaterials Program (DMR 0510138) and Ceramics Program (DMR 1006931).

REFERENCES

1. M.A. Meyers, P-Y. Chen, A.Y-M. Lin, and Y. Seki: Biological materials: Structure and mechanical properties. *Prog. Mater. Sci.* **53**, 1 (2008).
2. P-Y. Chen, A.Y-M. Lin, Y-S. Lin, Y. Seki, A.G. Stokes, J. Peyras, E.A. Olevsky, M.A. Meyers, and J. McKittrick: Structure and mechanical properties of selected biological materials. *J. Mech. Behav. Biomed. Mater.* **1**, 208 (2008).
3. A.Y-M. Lin and M.A. Meyers: Growth and structure in abalone shell. *Mater. Sci. Eng., A* **290**, 27 (2005).
4. M.A. Meyers, A.Y-M. Lin, P-Y. Chen, and J. Muyco: Mechanical strength of abalone nacre: Role of the soft organic layer. *J. Mech. Behav. Biomed. Mater.* **1**, 76 (2008).
5. P-Y. Chen, A.Y-M. Lin, J. McKittrick, and M.A. Meyers: Structure and mechanical properties of crab exoskeletons. *Acta Biomater.* **4**, 587 (2008).
6. J.C. Weaver, Q. Wang, A. Miserez, A. Tantuccio, R. Stromberg, K.N. Bozhilov, P. Maxwell, R. Nay, S.T. Heier, E. DiMasi, and D. Kisailus: Analysis of an ultra hard magnetic biomineral in chiton radular teeth. *Mater. Today* **13**, 42 (2010).
7. A. Miserez, T. Schneberk, C. Sun, F.W. Zok, and J.H. Waite: The transition from stiff to compliant materials in squid beaks. *Science* **318**, 1817 (2008).
8. M.A. Meyers, A.Y-M. Lin, Y-S. Lin, E.A. Olevsky, and S. Georgalis: The cutting edge: Sharp biological materials. *JOM* **60**, 19 (2008).
9. T. Atkins: *The Science and Engineering of Cutting* (Butterworth-Heinemann, Oxford, UK, 2009), p. 230.
10. J.M. Diamond: How great white sharks, saber-toothed cats and solders kill. *Nature* **322**, 773 (1986).
11. S.M. Snodgrass and P.W. Gilbert: A shark bite meter, in *Sharks, Skates and Rays*, edited by P.W. Gilbert, R.F. Mathewson, and D.P. Rall (The Johns Hopkins University Press, Baltimore, 1967) p. 331.
12. H. Onozato and N. Watabe: Studies on fish scale formation and resorption. *Cell Tissue Res.* **201**, 409 (1979).
13. L. Zylberberg and G. Nicolas: Ultrastructure of scales in a teleost (*Carassius auratus L.*) after use of rapid freeze-fixation and freeze-substitution. *Cell Tissue Res.* **223**, 349 (1982).

14. L. Zylberberg, J. Bereiter-Hahn, and J.Y. Sire: Cytoskeletal organization and collagen orientation in the fish scales. *Cell Tissue Res.* **253**, 597 (1988).
15. A. Bigi, M. Burghammer, R. Falconi, H.J. Koch, S. Panzavolta, and C. Riekel: Twisted plywood pattern of collagen in teleost scales: An x-ray diffraction investigation. *J. Struct. Biol.* **136**, 137 (2001).
16. T. Ikoma, H. Kobayashi, J. Tanaka, D. Walsh, and S. Mann: Microstructure, mechanical, and biomimetic properties of fish scales from *Pagrus major*. *J. Struct. Biol.* **142**, 327 (2003).
17. B.J.F. Bruet, J. Song, M.C. Boyce, and C. Ortiz: Materials design principles of ancient fish armor. *Nat. Mater.* **7**, 748 (2008).
18. F.G. Torres, O.P. Troncoso, J. Nakamatsu, C.J. Grande, and C.M. Gomez: Characterization of the nanocomposite laminate structure occurring in fish scales from Arapaima gigas. *Mater. Sci. Eng., C* **28**, 1276 (2008).
19. J. Song, C. Ortiz, and M.C. Boyce: Threat-protection mechanics of an armored fish. *J. Mech. Behav. Biomed. Mater.* **4**, 699 (2011).
20. Y-S. Lin, C-T. Wei, E.A. Olevsky, and M.A. Meyers: Mechanical properties and the laminate structure of Arapaima gigas scales. *J. Mech. Behav. Biomed. Mater.* **4**, 1145 (2011).
21. M.A. Meyers, Y-S. Lin, E.A. Olevsky, and P-Y. Chen: The scales of the Amazon arapaima: Bioinspiration for flexible ceramics. *Adv. Biomater.* (2011) (accepted).
22. J.D. Currey: Mechanical properties and adaptations of some less familiar bony tissues. *J. Mech. Behav. Biomed. Mater.* **3**, 357 (2010).
23. J. Daget, M. Gayet, F.J. Meunier, and J-Y. Sure: Major discoveries on the dermal skeleton of fossil and recent polypteriforms: A review. *Fish Fish.* **2**, 113 (2001).
24. W.C. Oliver and G.M. Pharr: An improved technique for determining hardness and elastic modulus using load and displacement sensing indentation experiments. *J. Mater. Res.* **7**, 1564 (1992).
25. J-Y. Rho, T.Y. Tsui, and G.M. Pharr: Elastic properties of human cortical and trabecular lamellar bone measured by nanoindentation. *Biomater.* **18**, 1325 (1997).
26. P.K. Zysset, X.E. Guo, C.E. Hoffler, K.E. Moore, and S.A. Goldstein: Elastic modulus and hardness of cortical and trabecular bone lamellae measured by nanoindentation in the human femur. *J. Biomech.* **32**, 1005 (1999).
27. J-Y. Rho, M.E. Roy II, T.Y. Tsui, and G.M. Pharr: Elastic properties of microstructural components of human bone tissue as measured by nanoindentation. *J. Biomed. Mater. Res.* **45A**, 48 (1999).
28. S. Hengsberger, A. Kulik, and P. Zysset: Nanoindentation discriminates the elastic properties of individual human bone lamellae under dry and physiological conditions. *Bone* **30**, 178 (2002).
29. Z. Fan and J-Y. Rho: Effects of viscoelasticity and time-dependent plasticity on nanoindentation measurements of human cortical bone. *J. Biomed. Mater. Res.* **67A**, 208 (2003).
30. D.M. Ebenstein, A. Kuo, J.J. Rodrigo, A.H. Reddi, M. Ries, and L. Pruitt: Nanoindentation technique for functional evaluation of cartilage repair tissue. *J. Mater. Res.* **19**, 273 (2004).
31. O. Franke, K. Durst, V. Maier, M. Göken, T. Birkholz, H. Schneider, F. Hennig, and K. Gelse: Mechanical properties of hyaline and repair cartilage studied by nanoindentation. *Acta Biomater.* **3**, 873 (2007).
32. O. Franke, M. Göken, M.A. Meyers, K. Durst, and A.M. Hodge: Dynamic nanoindentation of articular porcine cartilage. *Mater. Sci. Eng. C* **31**, 789 (2011).
33. B. van Meerbeek, G. Willems, J.P. Celis, J.R. Roos, M. Braerm, P. Lanbrechrs, and G. Vanherle: Assessment by nanoindentation of the hardness and elasticity of the resin-dentin bonding area. *J. Dent. Res.* **72**, 1434 (1993).
34. J.H. Kinney, M. Balooch, S.J. Marshall, G.W. Marshall, and T.P. Weihs: Hardness and Young's modulus of human peritubular and intertubular dentine. *Arch. Oral Biol.* **41**, 9 (1996).
35. H. Fong, M. Sarikaya, S.N. White, and M.L. Snead: Nano-mechanical properties profiles across dentin–enamel junction of human incisor teeth. *Mater. Sci. Eng., C* **7**, 119 (2000).
36. S. Habelitz, S.J. Marshall, G.W. Marshall, and M. Balooch: Mechanical properties of human dental enamel on the nanometre scale. *Arch. Oral Biol.* **46**, 173 (2001).
37. S. Habelitz, G.W. Marshall, M. Balooch, and S.J. Marshall: Nanoindentation and storage of teeth. *J. Biomech.* **35**, 995 (2002).
38. J.H. Kinney, S.J. Marshall, and G.W. Marshall: The mechanical properties of human dentin: A critical review and re-evaluation of the dental literature. *Crit. Rev. Oral Biol. Med.* **14**, 13 (2003).
39. F. Haque: Application of nanoindentation to development of biomedical materials. *Surf. Eng.* **19**, 255 (2003).
40. D.M. Ebenstein and L.A. Pruitt: Nanoindentation of biological materials. *Nano Today* **1**, 26 (2006).
41. L. Angker and M.V. Swain: Nanoindentation: Application to dental hard tissue investigations. *J. Mater. Res.* **21**, 1893 (2006).
42. M.L. Oyen: Nanoindentation hardness of mineralized tissues. *J. Biomech.* **39**, 2699 (2006).
43. O. Franke, M. Göken, and M.A. Hodge: The nanoindentation of soft tissue: Current and developing approaches. *JOM* **60**, 49 (2008).
44. M. Dickinson: Nanoindentation of biological composites. *IOP Conf. Ser.: Mater. Sci. Eng.* **4**, 012015 (2009).
45. M.L. Oyen: Nanoindentation of biological and biomimetic materials. *Exp. Tech.* (2011, in press).
46. H. Yao and H. Gao: Multi-scale cohesive laws in hierarchical materials. *Int. J. Solids Struct.* **45**, 3627 (2008).
47. L.B. Whitenack, D.C. Sinkins, Jr., P.J. Motta, M. Hirai, and A. Kumar: Young's modulus and hardness of shark tooth biomaterials. *Arch. Oral Biol.* **55**, 203 (2001).
48. V. Imbeni, J.J. Kruzic, G.W. Marshall, S.J. Marshall, and R.O. Ritchie: The dentin-enamel junction and the fracture of human teeth. *Nat. Mater.* **4**, 229 (2003).
49. E. Munch, M.E. Launey, D.H. Alsem, E. Saiz, A.P. Tomsia, and R.O. Ritchie: Tough bio-inspired hybrid materials. *Science* **322**, 1515 (2008).
50. M.E. Launey, E. Munch, D.H. Alsem, H.D. Barth, E. Saiz, A.P. Tomsia, and R.O. Ritchie: Designing highly toughened hybrid composites through nature-inspired hierarchical complexity. *Acta Mater.* **57**, 2919 (2009).